

Diffuse 0.5-1 keV X-Rays and Nuclear Gamma-Rays from Fast Particles in the Local Hot Bubble

Vincent Tatischeff and Reuven Ramaty
Laboratory for High Energy Astrophysics
Goddard Space Flight Center, Greenbelt, MD 20771

ABSTRACT

We show that interactions of fast particles with the boundary shell of the local hot bubble could make an important contribution to the 0.5-1 keV diffuse X-ray background observed with ROSAT. The bulk of these nonthermal X-rays are due to line emission from fast O ions of energies around 1 MeV/nucleon. This is the typical energy per particle in the ejecta of the supernova which is thought to have energized the bubble. We find that there is sufficient total energy in the ejecta to produce X-rays of the required intensity, subject to the details of the evolution of the fast particle population since the supernova explosion (about 3×10^5 years ago based on the age of the Geminga pulsar). The unequivocal signature of lines from deexcitations in fast ions is their large width ($\delta E/E \simeq 0.1$ for O lines), which will clearly distinguishes them from X-ray lines produced in a hot plasma.

If a small fraction of the total ejecta energy is converted into accelerated particle kinetic energy ($\gtrsim 30$ MeV/nucleon), the gamma-ray line emission produced in the boundary shell of the local hot bubble could account for the recently reported COMPTEL observations of nuclear gamma-ray lines from a broad region towards the Galactic center.

Subject headings: diffuse radiation–gamma rays: theory–ISM: bubbles–line: formation–supernovae: general–X-rays: ISM

1. INTRODUCTION

The origin of the diffuse X-ray background in the 0.5-1.0 keV range is not well understood. While at lower energies the background is most likely Galactic due to thermal emission from both the local hot bubble (LHB) and the Galactic halo (Snowden et al. 1998), at higher energies it is thought to be mostly extragalactic (e.g. Fabian & Barcons 1992). In the 0.5-1.0 keV energy range the X-ray background probably contains contributions from both the halo and extragalactic sources, but as the Galactic plane is optically thick in this energy range, these sources will be absorbed at low latitudes. Thus, the fact that the 0.5-1 keV background shows no strong absorption at low Galactic latitudes indicates that there are significant contributions in this energy range from relatively local Galactic sources (McCammon & Sanders 1990). However, the contributions of the $\sim 10^6$ K plasma in the LHB (Snowden et al. 1998) and of stellar sources (Schmitt and Snowden 1990) are insufficient to account for all of the observed 0.5-1 keV background.

In a previous paper we investigated in detail the X-ray line and continuum production from fast nonthermal ion interactions (Tatischeff, Ramaty, & Kozlovsky 1998; see also Ramaty, Kozlovsky, & Tatischeff 1997). We have shown that strong line emission is expected in the 0.5-1 keV energy range, mainly due to atomic deexcitations in fast O following electron capture and excitation. We applied these calculations to the Orion region from which nuclear gamma-ray lines were observed with COMPTEL (Bloemen et al. 1997a). In the present paper we investigate the contribution of nonthermal ion interactions in the LHB to the 0.5-1 keV diffuse X-ray background and calculate the nuclear gamma-ray line emission that is expected to accompany the X-rays.

2. THE 0.5-1 KEV X-RAY DIFFUSE BACKGROUND

We used the $\frac{3}{4}$ keV (0.47-1.2 keV) ROSAT all-sky survey data (Snowden et al. 1995). We have excluded regions from which we do not expect the observed X-rays to be produced predominantly by accelerated ions. We thus removed the quadrant $270^\circ < b^{II} < 60^\circ$ which contains the Sco-Cen bubble and a possible Galactic X-ray bulge (Park et al. 1997a; Snowden et al. 1997), as well as the Orion-Eridanus bubble, the Cygnus bubble, and the brightest point sources in the Galactic plane. The remaining longitude-averaged emission is shown in Figure 1a (vertical bars) as a function of Galactic latitude. We see that the distribution is quite smooth, with a mean count rate of $\sim 120 \times 10^{-6}$ counts s^{-1} arcmin^{-2} at high latitudes, slightly decreasing near the Galactic plane.

There are four established sources which contribute to the $\frac{3}{4}$ keV diffuse X-ray background (Figure 1a). We obtained the EXRB (extragalactic X-ray background) curve by extrapolating the power-law dependence of the background above 1 keV (Gendreau et al. 1995) to the $\frac{3}{4}$ keV band, and by taking into account photoelectric absorption employing the cross sections of Morrison & McCammon (1983), solar abundances, and the average latitude dependence of the Galactic atomic hydrogen from the Bell Laboratory survey (Stark et al. 1992; see also Snowden et al. 1990). The existence of extended soft X-ray emission from the Galactic halo was recently established

by Snowden et al. (1998) from X-ray shadowing observations in the ROSAT $\frac{1}{4}$ keV (0.12-0.284 keV) band. The halo emission corresponds to a plasma temperature of $\sim 10^6$ K and produces $\sim 1140 \times 10^{-6}$ counts s^{-1} arcmin $^{-2}$ and $\sim 410 \times 10^{-6}$ counts s^{-1} arcmin $^{-2}$ in the $\frac{1}{4}$ keV band, for the north and the south polar regions respectively. We calculate the contribution of this plasma to the $\frac{3}{4}$ keV band using the Raymond & Smith (1977) thermal emission model and the ROSAT response function (Snowden et al. 1994). Assuming an average of 1000×10^{-6} counts s^{-1} arcmin $^{-2}$ in the $\frac{1}{4}$ keV band for latitudes $b^{II} > 65^\circ$, we obtain 20×10^{-6} counts s^{-1} arcmin $^{-2}$ in the $\frac{3}{4}$ keV band at high latitudes. We derived the Galactic halo curve in Figure 1a by using this value and taking into account photoelectric absorption as for the EXRB.

The LHB is a cavity around the solar system filled with a rarefied ($\lesssim 5 \times 10^{-3}$ cm $^{-3}$) $\sim 10^6$ K plasma which accounts for all of the $\frac{1}{4}$ keV diffuse emission at low latitudes (exclusive of discrete emission features). Cox & Anderson (1982) have successfully modeled the observed $\frac{1}{4}$ keV X-ray intensity by the reheating of a pre-existing cavity by a supernova blast wave containing $\sim 5 \times 10^{50}$ ergs. It was suggested that the Geminga pulsar is the remnant of this supernova that occurred $\sim 3 \times 10^5$ years ago, based on the age of the pulsar (Gehrels and Chen 1993). The radius of the LHB inferred from the ROSAT $\frac{1}{4}$ keV observations ranges from about 40 to 90 pc along the Galactic plane and from about 50 to 130 pc at high latitudes (Snowden et al. 1998). We approximate this cavity by an ellipsoid of revolution centered on the Sun with radius of 50 pc along the minor axis in the Galactic plane and 75 pc along the major axis perpendicular to the plane. In the displacement model (Sanders et al. 1977), which was shown to be consistent with the available data, the X-ray intensity is proportional to the radius of the cavity. Snowden et al. (1998) have established a scale factor of 0.155 pc $(10^{-6}$ counts s^{-1} arcmin $^{-2})^{-1}$ for the $\frac{1}{4}$ keV band. Using again the Raymond & Smith (1977) model and the ROSAT response function, we derived for this 10^6 K plasma a scale factor of 27.7 pc $(10^{-6}$ counts s^{-1} arcmin $^{-2})^{-1}$ in the $\frac{3}{4}$ keV band. For our assumed ellipsoidal shape of the LHB (100 pc minor axis and 150 pc major axis) we obtain the LHB curve in Figure 1a which, as can be seen, contributes less than 3% to the observed $\frac{3}{4}$ keV band intensity. As the estimated average H column density within the LHB is less than $\sim 5 \times 10^{18}$ cm $^{-2}$ (Bloch et al. 1986; Juda et al. 1991), we can safely neglect absorption for both the $\frac{1}{4}$ keV and $\frac{3}{4}$ keV bands. We estimated the unresolved stellar contribution (the dM stars curve in Figure 1a) by scaling the curve in McCammon & Sanders (1990, figure 8) to the ROSAT data (vertical bars in Figure 1a).

We see in Figure 1a that the total emission resulting from these four sources accounts for only $\sim 70\%$ of the observed intensity at high latitudes and for less than 20% in the Galactic plane, thus requiring a significant contribution from sources within our Galaxy. The filled squares in Figure 1b show the required residual emission obtained by subtracting the total emission of the four established source distributions from the observed intensity in Figure 1a. While at high latitudes this residual emission could be extragalactic (e.g. Cen et al. 1995), or originate from the halo, a Galactic component is clearly needed to explain the residual emission in the plane. We now investigate the possibility that the excess $\frac{3}{4}$ keV emission is entirely Galactic resulting from

fast ion interactions.

3. X-RAY AND GAMMA-RAY PRODUCTION

We assume that the X-ray production takes place in the boundary shell of the LHB. The observed X-ray flux per unit solid angle can then be written as

$$\frac{d\Phi_x}{d\Omega} = \frac{1}{4\pi D^2} \frac{dQ_x}{d\Omega}. \quad (1)$$

Here $dQ_x/d\Omega$ is the emission produced in a volume of the shell bounded by the solid angle element $d\Omega$ (as viewed from the Earth), and $D^2 = \int_{r_1}^{r_2} q_x r^2 dr / \int_{r_1}^{r_2} q_x dr$ is a mean square distance determined by the distribution of the X-ray emissivity q_x and the shell thickness $(r_2 - r_1)$. We assume that at $\frac{3}{4}$ keV absorption within the shell can be neglected. By further assuming that $dQ_x/d\Omega$ is independent of the direction of observation Ω , we obtain the solid curve in Figure 1b, where the root mean square distance D was allowed to trace out the above defined ellipsoid (radii of 50 and 75 pc in the plane and perpendicular to the plane, respectively). This curve is, for now, arbitrarily normalized to the data.

As the bulk of the nonthermal $\frac{3}{4}$ keV emission is line emission from fast O ions of typical energies around 1 MeV/nucleon (Tatischeff et al. 1998), we first consider a scenario in which the fast particles are the ejecta of the supernova which is thought to have energized the LHB. As the most efficient X-ray line production will result from fast particles enriched in heavy ions (mostly O), we assume that the progenitor of the supernova in question was a massive star which has lost its H and He envelope. We thus derive the spectrum of the fast ions below 2 MeV/nucleon using the velocity distribution of the ejected mass ($2.85 M_\odot$) of a supernova resulting from a $60 M_\odot$ progenitor (Woosley, Langer, & Weaver 1993, figure 9). Above 2 MeV/nucleon, we extrapolate the particle spectrum with an E^{-4} energy dependence (Fields et al. 1996), which is consistent with the ejected masses at speeds in excess of 2×10^4 and 3×10^4 km s $^{-1}$ given by Woosley et al. (1993). The result is shown by the solid curve in Figure 2, where we plot the differential energy content in the ejecta, i.e the energy content per unit kinetic energy per nucleon E . Since the production of the nonthermal $\frac{3}{4}$ keV X-rays is independent of any cutoff in the ejecta energy spectrum above 2 MeV/nucleon, we extend the spectrum to infinity.

We calculated the production of X-rays by fast ions with energy spectrum given by the SN60 curve in Figure 2 and composition of the ejecta given by Woosley et al. (1993, table 4). We allowed these ions to impinge upon the boundary shell of the LHB, assuming a steady state, thick target interaction model (Tatischeff et al. 1998) with a neutral ambient medium of solar composition. The assumption that the X-rays are not absorbed in the shell requires that the H column depth through the shell be $\lesssim 3 \times 10^{20}$ cm $^{-2}$. Such a H column is sufficient to slow down a 2 MeV/nucleon O to about 1 MeV/nucleon. Since the bulk of the X-ray line emission from fast O ions takes place between 0.4 and 2 MeV/nucleon (Tatischeff et al. 1998), the assumption of

a thick target for the fast particles is not unreasonable because magnetic fields within the shell could confine the particles to longer paths than simple straight line trajectories through the shell. We used the SN60 spectrum in Figure 2 with a renormalization to a power deposition \dot{W} such that the calculated $\frac{3}{4}$ keV count rate for a distance $D=50$ pc [Eq. (1)] in the Galactic plane equals 60×10^{-6} counts s^{-1} arcmin $^{-2}$ (the required emission to account for this background in the plane, Figure 1b). We obtain $\dot{W}=2.6 \times 10^{38}$ erg s^{-1} , which is the power required to produce the total X-ray emission in the shell $\int (dQ_x/d\Omega)d\Omega$ [see Eq. (1)]. This power integrated over 2×10^5 years (comparable to the age of the Geminga pulsar) yields a total energy equal to the initial energy of the ejecta, $\sim 1.5 \times 10^{51}$ erg. We thus conclude that it is possible that the required fraction of the $\frac{3}{4}$ keV background (Figure 1) is indeed due to nonthermal interactions of the supernova ejecta.

The corresponding X-ray spectrum, shown in Figure 3, is obtained by using our nonthermal X-ray production code (Tatischeff et al. 1998). We see that the $\frac{3}{4}$ keV band (0.47-1.2 keV) is dominated by the broad He-like O lines at 0.57 and 0.67 keV, with some contribution from H-like O at 0.65 keV. These lines, as well as the various other broad lines seen in Figure 3, are due to atomic deexcitations in the fast ions following electron capture and excitation. The narrow lines (e.g. the Fe lines at 6.4 and 7.06 keV) are due to K-shell vacancy production in the ambient atoms by the fast ions. The continuum is due to inverse bremsstrahlung and secondary electron bremsstrahlung.

We also calculated the gamma-ray line production in the 3-7 MeV energy band (Ramaty, Kozlovsky, & Lingenfelter 1996) due to the fastest particles of the supernova ejecta, again assuming a thick target interaction model. In the Galactic plane we obtain $\Phi_{3-7}=2.4 \times 10^{-6}$ photons cm^{-2} s^{-1} sr^{-1} which is much smaller than the COMPTEL flux ($\sim 1.5 \times 10^{-4}$ photons cm^{-2} s^{-1} sr^{-1}) from a broad region in the direction of the Galactic center (Bloemen et al. 1997b). We thus see that the fast particles of the supernova ejecta, while potentially capable of producing very interesting fluxes of X-ray line emission, cannot play any significant role in nuclear gamma-ray line production. This result also shows that supernova ejecta without further acceleration cannot lead to sufficient gamma-ray line production to account for the COMPTEL observations of Orion (Cameron et al. 1995; Fields et al. 1996; Tatischeff et al. 1996). This is because for the steep spectra of the ejecta the accompanying X-ray production would greatly exceed the ROSAT upper limits (Tatischeff et al. 1998).

Since it is possible that the fast particles of the supernova ejecta lose their energy on a time scale shorter than $\sim 3 \times 10^5$ years (the elapsed time since the supernova explosion), we also consider an alternative scenario in which both the X-rays and gamma rays are produced by accelerated particles. For generality, we specify neither the acceleration mechanism nor the acceleration time or site. We simply assume the spectrum that was used to calculate gamma-ray line emission in Orion (Ramaty et al. 1996),

$$\frac{d\Phi}{dE} \propto E^{-1.5} e^{-E/E_0}, \quad (2)$$

which could result from shock acceleration. Employing the same steady state, thick target

interaction model (Ramaty et al. 1996; Tatischeff et al. 1998) as we used for the supernova ejecta spectrum, we calculate both the X-ray and gamma-ray emissions using Eq. (2) and the SN60 ejecta composition (Woosley et al. 1993). The solid curve in Figure 4 shows the 3-7 MeV nuclear gamma-ray line flux that is expected to accompany the X-ray production that yields 60×10^{-6} counts s^{-1} arcmin^{-2} in the ROSAT PSPC $\frac{3}{4}$ keV band. The dashed horizontal line is the COMPTEL flux from the direction of the Galactic center, mentioned above. Taking this flux as an upper limit, we conclude that if the $\frac{3}{4}$ keV X-ray background were due to accelerated particles [Eq. (2)], their energy spectrum must be soft enough ($E_0 \lesssim 10$ MeV/nucleon) in order not to overproduce the nuclear gamma-ray line emission. The dashed curve in Figure 4 is the power deposition \dot{W} that accompanies X-ray production in the entire boundary shell leading to a $\frac{3}{4}$ keV count rate of 60×10^{-6} counts s^{-1} arcmin^{-2} for a distance of 50 pc. We see that the most efficient X-ray production is for $2 \lesssim E_0 \lesssim 10$ MeV/nucleon for which $\dot{W} \simeq 2 \times 10^{38}$ erg s^{-1} , essentially the same as the power deposition for the supernova ejecta spectrum.

Finally we consider a hybrid model incorporating both the fast particles of the supernova ejecta and accelerated particles with spectrum given by Eq. (2). We have normalized the supernova ejecta spectrum so that it by itself yields the required ROSAT $\frac{3}{4}$ keV count rate for a distance of 50 pc. This implies the power deposition of 2.6×10^{38} erg s^{-1} given above. We then normalized the shock acceleration spectrum to a power deposition equal to 20% of this value. For the same integration time of 2×10^5 years used above, we obtain the shock acceleration spectra shown by the dashed curves in Figure 2.

The sum of the contributions from the two spectral components are shown in Table 1, for $E_0=10, 30$ and 100 MeV/nucleon. The $E_0=0$ case represents only the supernova ejecta contribution without additional particle acceleration and $E_0=100$ MeV/nucleon is an upper limit derived for Orion (Tatischeff, Ramaty, Mandzhavidze 1997) using EGRET gamma-ray data. We see that, while the contribution of the shock spectrum to the X-ray line production is small, it dominates the gamma-ray line production. Thus, for $E_0=100$ MeV/nucleon we can account for the observed COMPTEL flux with a power deposition of only 5.2×10^{37} erg s^{-1} in the entire boundary shell. But if the nuclear gamma-ray lines are produced in only part of the boundary shell (1.5 sr, Bloemen et al. 1997b) the power deposition could be as small as 2% of that required for the production of the $\frac{3}{4}$ keV background.

4. DISCUSSION AND CONCLUSIONS

We have shown that X-rays produced by fast ions could make an important contribution to the 0.5-1 keV diffuse X-ray background. The bulk of the emission in this energy range is due to line emission following electron capture and excitation in fast O ions of ~ 1 MeV/nucleon. A promising source for these particles is the ejecta of the supernova which energized the LHB, and conceivably gave rise to the Geminga pulsar (Gehrels & Chen 1993). The unequivocal signature of lines from deexcitations in fast ions is their large width ($\delta E/E \simeq 0.1$ for O lines), which could clearly

distinguish them from the X-ray lines produced in a hot plasma. O line emission has already been observed in the diffuse X-ray background (e.g. Rocchia et al. 1984), but the resolution of the solid-state detectors (~ 150 eV FWHM) is not sufficient to make the distinction.

For the calculation of the X-ray production we adopted a model in which the fast ions interact in the boundary shell of the LHB. Since this shell is probably more inhomogeneous than the hot plasma within the bubble, we expect significant spatial variation of the 0.5-1 keV background. Small-scale variations in the $\frac{1}{4}$ keV background have already been observed, suggesting emission associated with the boundary shell (Park, Finley, & Snowden 1997b). Further information on the validity of our model could be obtained from observations of X-ray shadows due to molecular clouds, such as the observations of Kuntz, Snowden, & Verter (1997).

We have also calculated the gamma-ray line emission in the 3-7 MeV energy range, which is due mostly to nuclear deexcitations in C and O. We showed that the gamma-ray line emission produced by the fast supernova ejecta is unobservable with current instruments. However, if a significant fraction (at least 2%) of the ejecta energy is converted into accelerated particle kinetic energy, the gamma-ray line emission produced in the local hot bubble could account for the recent COMPTEL observations (Bloemen et al. 1997b) from a broad region towards the Galactic center. Such local production could provide an explanation to the broad latitude extend of this emission.

We wish to acknowledge useful discussions with Steve Snowden. V. T. acknowledges an NRC Research Associateship at the Goddard Space Flight Center.

REFERENCES

- Bloch, J. J., Jahoda, K., Juda, M., McCammon, D., Sanders, W. T., & Snowden, S. L. 1986, *ApJ*, 308, L59
- Bloemen, H., et al. 1997a, *ApJ*, 475, L25
- Bloemen, H., et al. 1997b, *Proc. 4th Compton Symposium*, (AIP: New York), vol.2, 1074
- Cameron, A. G. W., Höflich, P., Meyers, P. C., & Clayton, D. D. 1995, *ApJ*, 447, L53
- Cen, R., Kang, H., Ostriker, J. P., & Ryu, D. 1995, *ApJ*, 451, 436
- Cox, D. P., & Anderson, P. R. 1982, *ApJ*, 253, 268
- Fabian, A. C., & Barcons, X. 1992, *ARA&A*, 30, 429
- Fields, B. D., Cassé, M., Vangioni-Flam, E., & Nomoto, K. 1996, *ApJ*, 462, 276
- Gendreau, K. C., et al. 1995, *Publ. Astron. Soc. Japan*, 47, L5
- Gehrels, N., & Chen, W. 1993, *Nature*, 361, 706

- Juda, M., Bloch, J. J., Edwards, B. C., McCammon, D., Sanders, W. T., Snowden, S. L., & Zhang, J. 1991, *ApJ*, 367, 182
- Kuntz, K. D., Snowden, S. L., & Verter, F. 1997, *ApJ*, 484, 245
- McCammon, D., & Sanders, W. T. 1990, *ARA&A*, 28, 657
- Morrison, R., & McCammon, D. 1983, *ApJ*, 270, 119
- Park, S., Finley, J. P., Snowden, S. L., & Dame, T. M. 1997a, *ApJ*, 476, L77
- Park, S., Finley, J. P., & Snowden, S. L. 1997b, *ApJ*, 491, 165
- Ramaty, R., Kozlovsky, B., & Lingenfelter, R. E. 1996, *ApJ*, 456, 525
- Ramaty, R., Kozlovsky, B., & Tatischeff, V. 1997, *Proc. 4th Compton Symposium*, (AIP: New York), vol.2, 1049
- Raymond, J. C., & Smith, B. M. 1977, *ApJS*, 35, 419
- Rocchia, R., et al. 1984, *A&A*, 130, 53
- Sanders, W. T., Kraushaar, W. L., Nousek, J. A., & Fried, P. M. 1977, *ApJ*, 217, L87
- Schmitt, J. H. M. M., & Snowden, S. L. 1990, *ApJ*, 361, 207
- Snowden, S. L., Cox, D. P., McCammon, D., & Sanders, W. T. 1990, *ApJ*, 354, 211
- Snowden, S. L., McCammon, D., Burrows, D. N., & Mendenhall, J. A. 1994, *ApJ*, 454, 643
- Snowden, S. L., et al. 1995, *ApJ*, 454, 643
- Snowden, S. L., et al. 1997, *ApJ*, 485, 125
- Snowden, S. L., Egger, R., Finkbeiner, D. P., Freyberg, M. J., & Plucinsky, P. P. 1998, *ApJ*, 493, 715
- Stark, A. A., Gammie, C. F., Wilson, R. W., Bally, J., Linke, R. A., Heiles, C., & Hurwitz, M. 1992, *ApJS*, 79, 77
- Tatischeff, V., Cassé, M., Kiener, J., Thibaud, J.-P., & Vangioni-Flam, E. 1996, *ApJ*, 472, 205
- Tatischeff, V., Ramaty, R., & Mandzhavidze, N. 1997, *Proc. 4th Compton Symposium*, (AIP: New York), vol.2, 1054
- Tatischeff, V., Ramaty, R., & Kozlovsky, B. 1998, *ApJ*, in press
- Woosley, S. E., Langer, N., & Weaver, T. A. 1993, *ApJ*, 411, 823

Table 1. Predicted X-ray and gamma-ray emissions at low latitudes^a

E_0 (MeV/nucl)	X-ray ^b	Gamma-ray ^c
0 ^d	60.0	0.024
10	74.5	0.22
30	71.0	0.70
100	67.3	1.43

^aFor a combination of the SN60 and shock spectra of Figure 2 and a distance to the emission source [Eq. (1)] $D=50$ pc. The SN60 and shock spectra are normalized to powers of 2.6×10^{38} and 5.2×10^{37} erg s⁻¹, respectively.

^bIn units of 10^{-6} counts s⁻¹ arcmin⁻² in the ROSAT PSPC $\frac{3}{4}$ keV band.

^cIn units of 10^{-4} photons cm⁻² s⁻¹ sr⁻¹ in the 3-7 MeV energy range.

^dSupernova ejecta without additional particle acceleration.

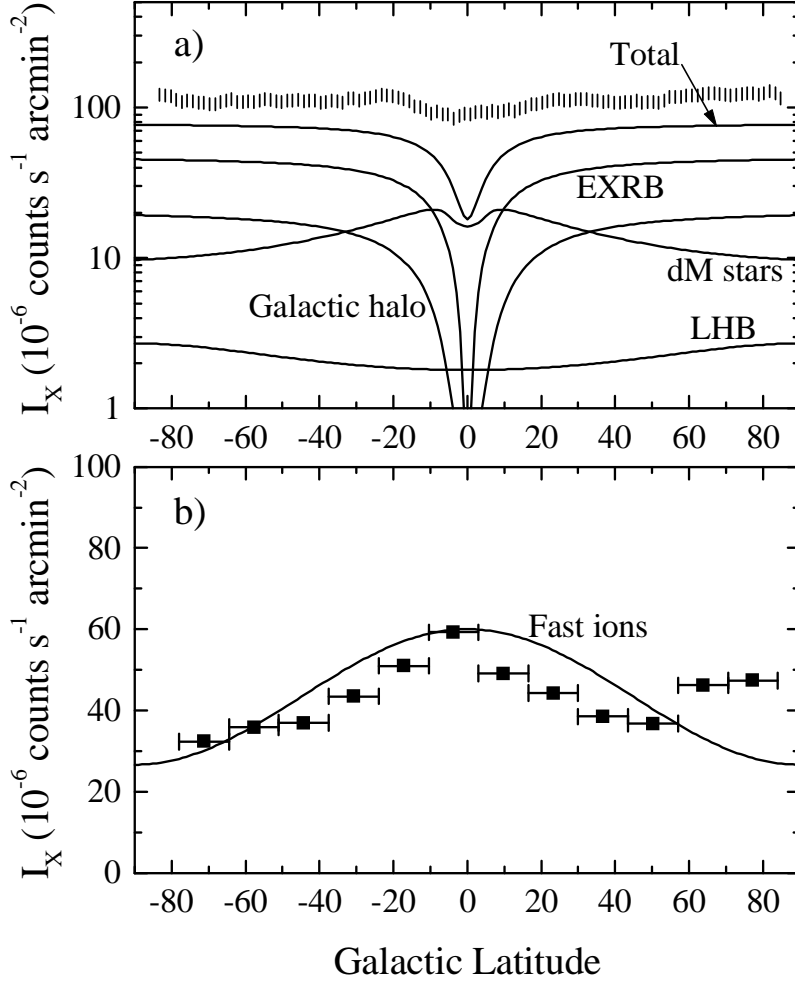


Fig. 1.— Longitude averaged $\frac{3}{4}$ keV diffuse X-ray background components as functions of Galactic latitude. Panel (a): vertical bars – total ROSAT PSPC emission; total solid curve – sum of contributions from the extragalactic X-ray background (EXRB), late-type dwarf stars, the Galactic halo and the local hot bubble. Panel (b): filled squares – residual emission after subtraction of the total curve in panel (a) from the data, averaged over 13.5° bins; solid curve – X-ray emission from fast ion interactions with the boundary shell of the LHB (see text).

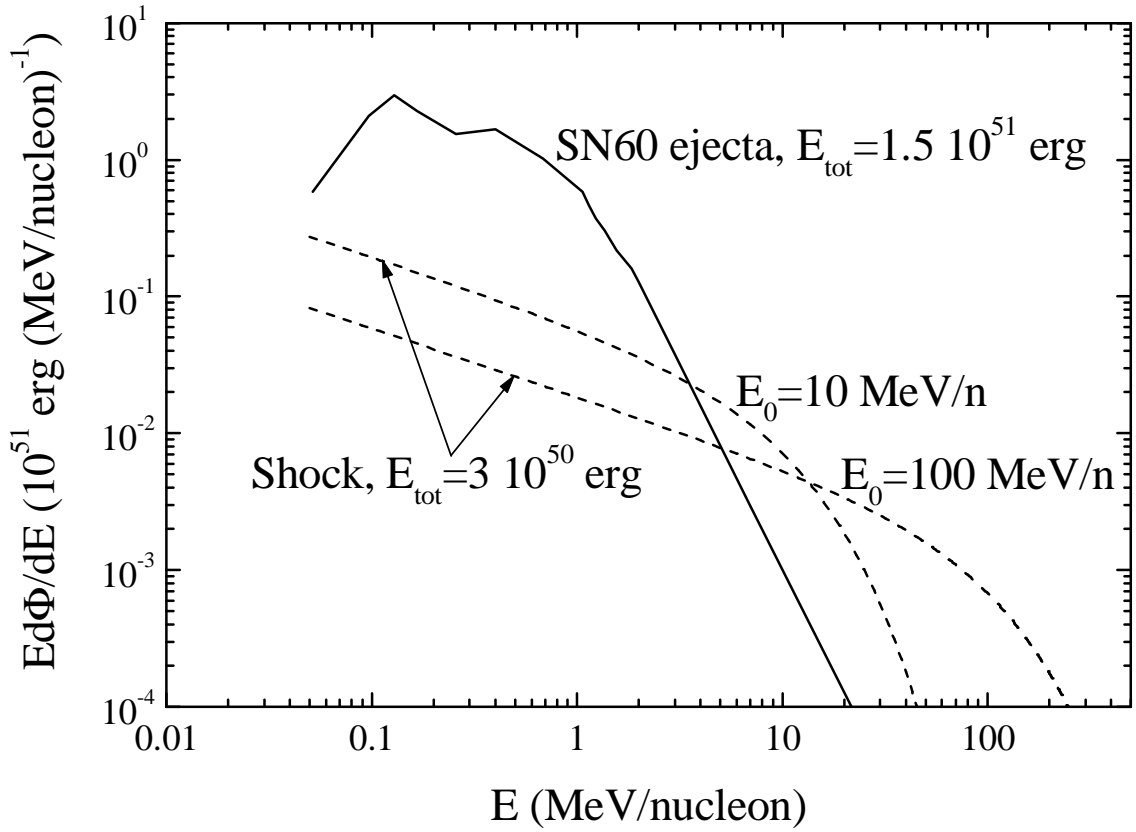


Fig. 2.— Fast particle differential energy contents. Solid curve – ejecta of a supernova resulting from a $60 M_{\odot}$ progenitor (Woosley et al. 1993) containing 1.5×10^{51} erg; dashed curves – shock acceleration spectra [Eq. (2)] normalized to a total accelerated particle kinetic energy content of 20% of that of the ejecta.

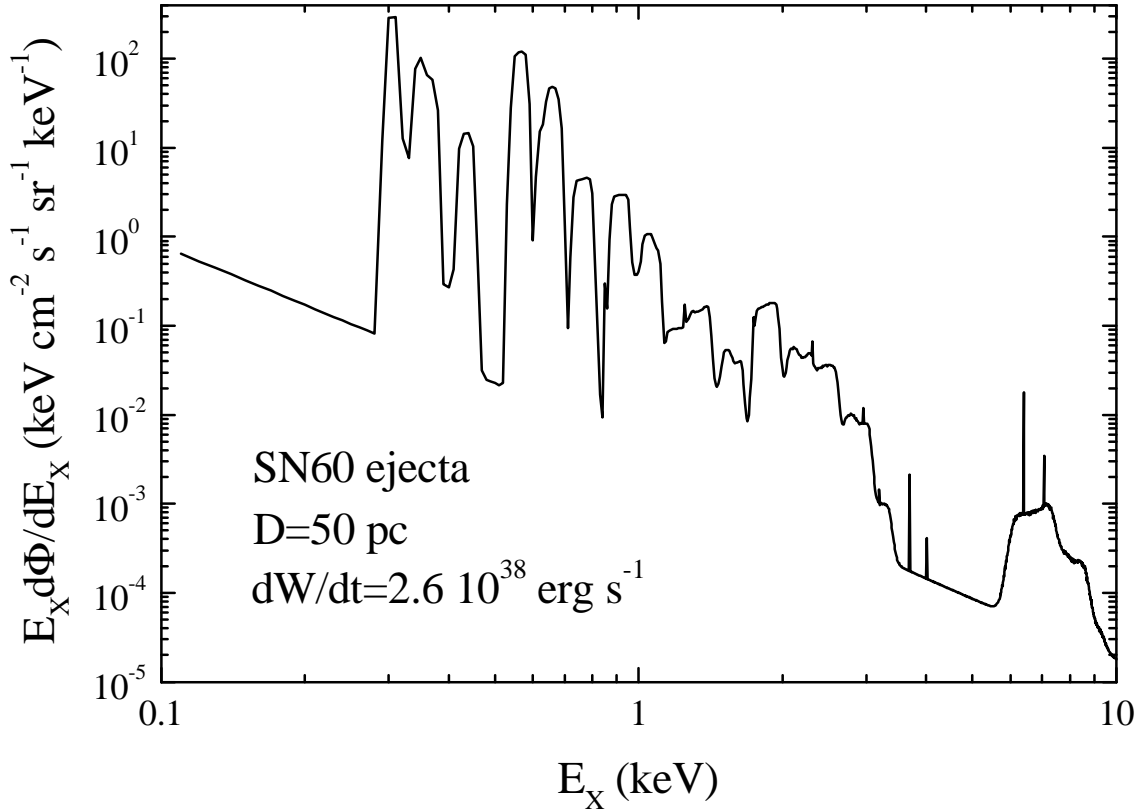


Fig. 3.— X-ray emission produced by the ejecta of a supernova from a $60 M_{\odot}$ progenitor (Woosley et al. 1993) interacting in the boundary shell of the LHB. The calculation is normalized to a total power of 2.6×10^{38} erg s $^{-1}$ deposited in the shell by the ejecta, yielding 60×10^{-6} counts s $^{-1}$ arcmin $^{-2}$ in the ROSAT PSPC $\frac{3}{4}$ keV band for a distance of 50 pc.

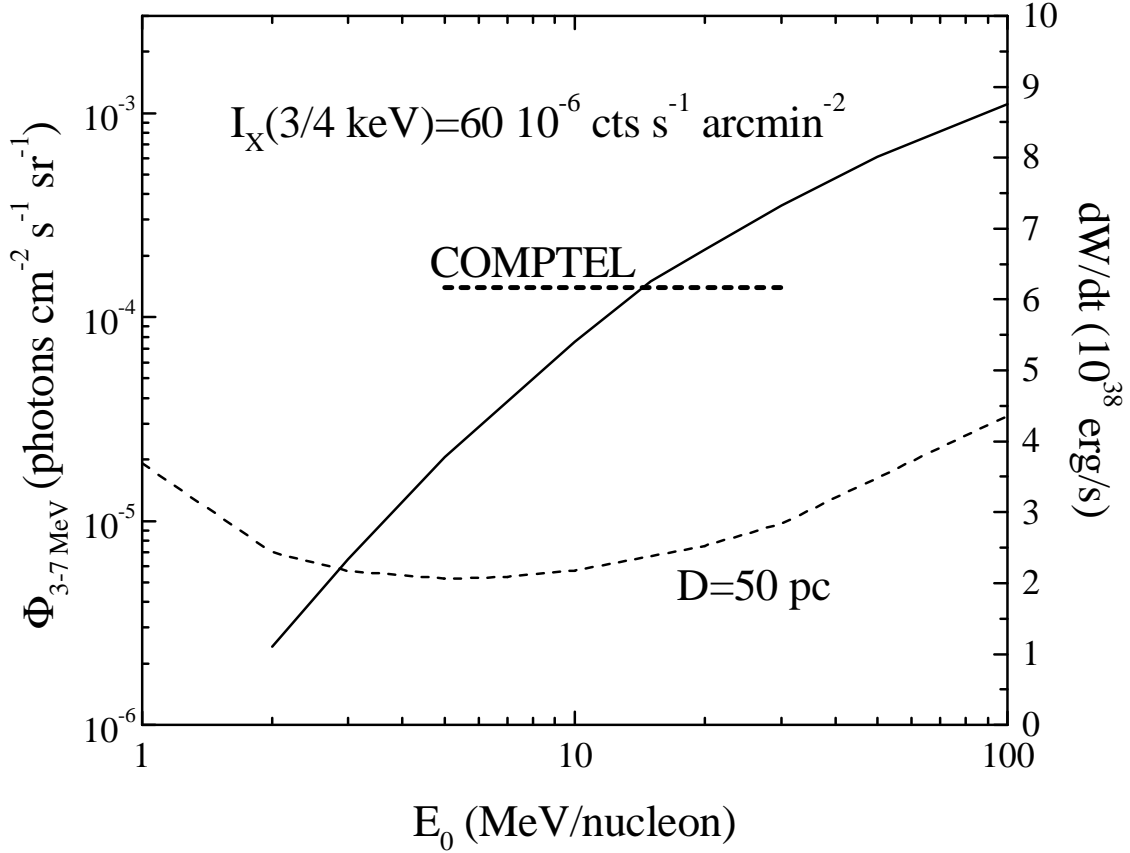


Fig. 4.— Solid curve – nuclear gamma-ray line emission in the 3-7 MeV energy range (left vertical axis) that accompanies the X-ray production by the shock acceleration spectrum (Figure 2) as a function of E_0 [Eq. (2)]. The calculation is normalized to an X-ray production of 60×10^{-6} counts s^{-1} arcmin^{-2} in the ROSAT PSPC $\frac{3}{4}$ keV band. Also shown is the COMPTEL flux from a broad region in the direction of the Galactic center (Bloemen et al. 1997b). Dashed curve – total power deposited in the shell by the accelerated ions (right vertical axis) as a function of E_0 . The calculation is normalized to provide the same X-ray production in the $\frac{3}{4}$ keV band for a distance of 50 pc.